JVI Journals.ASM.org

Canine Distemper Virus Epithelial Cell Infection Is Required for Clinical Disease but Not for Immunosuppression

Bevan Sawatsky,[a]* Xiao-Xiang Wong,[a] Sarah Hinkelmann,[b] Roberto Cattaneo,[c] and Veronika von Messling[a,d]

INRS-Institut Armand-Frappier, University of Quebec, Laval, Canada[a]; Institute for Virology, Veterinary School Hannover, Hannover, Germany[b]; Department of Molecular Medicine, Virology and Gene Therapy Track, Mayo Clinic College of Medicine, Rochester, Minnesota, USA[c]; and Emerging Infectious Diseases Program, Duke-NUS Graduate Medical School Singapore, Singapore, Singapore[d]

To characterize the importance of infection of epithelial cells for morbillivirus pathogenesis, we took advantage of the severe disease caused by canine distemper virus (CDV) in ferrets. To obtain a CDV that was unable to enter epithelial cells but retained the ability to enter immune cells, we transferred to its attachment (H) protein two mutations shown to interfere with the interaction of measles virus H with its epithelial receptor, human nectin-4. As expected for an epithelial receptor (EpR)-blind CDV, this virus infected dog and ferret epithelial cells inefficiently and did not cause cell fusion or syncytium formation. On the other hand, the EpR-blind CDV replicated in cells expressing canine signaling lymphocyte activation molecule (SLAM), the morbillivirus immune cell receptor, with similar kinetics to those of wild-type CDV. While ferrets infected with wild-type CDV died within 12 days after infection, after developing severe rash and fever, animals infected with the EpR-blind virus showed no clinical signs of disease. Nevertheless, both viruses spread rapidly and efficiently in immune cells, causing similar levels of leukopenia and inhibition of lymphocyte proliferation activity, two indicators of morbillivirus immunosuppression. Infection was documented for airway epithelia of ferrets infected with wild-type CDV but not for those of animals infected with the EpR-blind virus, and only animals infected with wild-type CDV shed virus. Thus, epithelial cell infection is necessary for clinical disease and efficient virus shedding but not for immunosuppression.

Morbilliviruses are highly contagious and can cause severe disease in their respective hosts. *Measles virus* (MeV), which infects humans and certain nonhuman primates, is generally associated with mild to moderate clinical signs (5), while the closely related *Canine distemper virus* (CDV) infects a broad range of carnivores and causes severe and frequently lethal disease (2). Upon aerosol transmission, these viruses initially target signaling lymphocyte activation molecule (SLAM; CD150)-expressing immune cells in the respiratory tract (6, 11), followed by dissemination throughout the lymphatic system (4, 33). SLAM proteins from different host species serve as receptors for multiple morbilliviruses (31), and the amino acid residues involved in the interaction of the MeV and CDV attachment (H) proteins with SLAM are structurally conserved (32, 34). The importance of immune cell targeting for the establishment of morbillivirus infection is illustrated by the complete attenuation of SLAM-binding-defective MeV and CDV *in vivo*, despite their ability to infect and replicate in nonimmune cells as efficiently as wild-type viruses *in vitro* (12, 36).

In contrast, the role of epithelial cell tropism in morbillivirus pathogenesis is less clear. Infection of epithelia coincides with the development of the characteristic rash and respiratory and gastrointestinal signs of disease, and the extent of dissemination correlates with the severity of clinical signs (15, 33). MeV H protein residues critical for infection of epithelial cells have been identified (13, 29), and these residues are important for binding to nectin-4, the recently identified MeV epithelial receptor (17, 19). Pathogenesis of a nectin-4-blind MeV in rhesus macaques was similar to that of the parental wild-type strain, although no virus shedding into the airways was observed (13). However, since MeV-induced disease in monkeys was generally mild and short-lived, it was difficult to assess how relevant infection of epithelial tissues is for disease and pathogenesis.

Because of the more severe disease caused by CDV in ferrets, this animal model is ideal for characterizing morbillivirus pathogenesis mechanisms (24). A recent study demonstrated that several of the amino acids that are involved in nectin-4 binding of MeV H are also important for CDV epithelial cell entry (10, 13), indicating that similar to immune cell entry via SLAM, the mechanism of epithelial cell infection may be conserved among morbilliviruses. We therefore transferred mutations conferring the nectin-4-blind phenotype to MeV H into the H protein of a lethal CDV strain. After *in vitro* characterization of the mutant H proteins, we generated a candidate epithelial receptor (EpR)-blind virus and confirmed that it was unable to infect canine and ferret epithelial cells. The pathogenesis and tropism of this virus were then characterized in ferrets.

MATERIALS AND METHODS

Cells and transfections. Vero cells constitutively expressing canine SLAM (VerodogSLAMtag cells) (35), 293 cells (ATCC CRL-1573), Madin-Darby canine kidney (MDCK) cells (ATCC CCL-34), and ferret alveolar epithelial cells (FtAEpCs) (9) were maintained in Dulbecco's modified Eagle medium (DMEM; Gibco) supplemented with 5% heat-inactivated fetal bovine serum (FBS). For the biochemical analysis of recombinant proteins, 12-well plates of VerodogSLAMtag cells were transfected at ap-

Received 26 September 2011 Accepted 3 January 2012

Published ahead of print 25 January 2012

Address correspondence to Veronika von Messling, veronika.vonmessling@duke-nus.edu.sg.

* Present address: University of Texas Medical Branch, Department of Microbiology and Immunology, Galveston, Texas, USA.

doi:10.1128/JVI.06414-11

proximately 90% confluence as described previously (26, 27). Briefly, each well was transfected with 2 μg each of the H expression plasmid pCG-H5804Pzeo (34) or the respective mutant H plasmid and a plasmid expressing either the MeV Edmonston (3) or CDV 5804P F protein by use of Turbofect (Fermentas). Fusion activity was evaluated after 24 h. Alternatively, cells were lysed in 200 μl of RIPA buffer (50 mM Tris-HCl, pH 8.0, 150 mM NaCl, 1% NP-40, and 0.5% sodium deoxycholate) containing a protease inhibitor cocktail (Complete; Roche) 16 h after transfection. The lysate was centrifuged at 14,000 rpm for 15 min at 4°C and stored at −20°C.

Production of EpR/nectin-4-blind CDV and MeV H proteins. To generate EpR-blind CDV H proteins, site-directed mutagenesis was performed on the plasmid pCG-H5804PZeo (34) to introduce the mutations V478S, P493S, and Y539A, as well as the double mutation P493S/Y539A. These mutations correspond to those reported by Leonard et al. (13), taking into account the four additional amino acids present upstream of that region in MeV H (34). The nectin-4-blind MeV H protein expression plasmids for the L482S, P497S, Y543A, and P497S/Y543A mutants were generated by site-directed mutagenesis of the plasmid pcDNA3.1-MeV H_{IC323} (13, 30).

To generate the recombinant virus p5804PeH$_{EpR\text{-}blind}$, the P497S/Y543A double mutation was first introduced into a subgenomic plasmid containing the region between the BsrGI and AscI restriction sites. Using these restriction sites, the fragment was then transferred into the full-length p5804PeH plasmid, which expresses enhanced green fluorescent protein (EGFP) from an additional open reading frame located between the H and polymerase genes (33). All plasmids were verified by sequencing.

Recovery of recombinant virus and growth kinetics. The recombinant EpR-blind CDV was recovered by transfecting semiconfluent 293 cells with 6 μg of p5804PeH$_{EpR\text{-}blind}$ and a combination of 0.5, 0.1, 0.5, and 0.7 μg MeV N, P, and polymerase (L) and T7 RNA polymerase expression plasmids (1, 14), respectively, using Turbofect (Fermentas). Three days later, the transfected cells were transferred onto VerodogSLAMtag cells seeded at 80 to 90% confluence in 10-cm dishes. Individual syncytia were inoculated on fresh VerodogSLAMtag cells. Stocks of all viruses used in this study were produced on VerodogSLAMtag cells. Titers were determined by limiting dilution and expressed as 50% tissue culture infective doses ($TCID_{50}$).

For growth kinetics, VerodogSLAMtag and MDCK cells and FtAEpCs were plated in 24-well plates and infected at a multiplicity of infection (MOI) of 0.1 or 0.01. For VerodogSLAMtag cells, cells were scraped into the supernatant and harvested daily for 4 days; for MDCK cells and FtAEpCs, samples were harvested every second day for 8 days. Titers were determined by a limiting dilution method and expressed as $TCID_{50}$. Phase-contrast and fluorescence pictures were taken on the days of harvest.

Cell surface biotinylation and Western blot analysis. For cell surface biotinylation, transfected cells were incubated for 20 min at 4°C with EZ-Link *N*-hydroxysuccinimide (NHS)-LC-LC-biotin (Pierce) at a concentration of 2 mM in phosphate-buffered saline (PBS) and then washed with 100 mM glycine in PBS (Invitrogen) to quench excess biotin. The cells were then lysed with RIPA buffer with protease inhibitors, and a 20-μl aliquot of each sample was mixed directly with an equal volume of 2× SDS gel loading buffer (SDS-GLB) containing 10% β-mercaptoethanol and stored at −20°C. The remaining lysate was mixed with immobilized protein G Plus beads (Santa Cruz) and a rabbit anti-peptide antiserum raised against the cytoplasmic tail (Hcyt) of the respective H protein (37). After agitation overnight at 4°C, samples were washed three times, mixed with 1× SDS-GLB, and heated at 75°C for 5 min. The immunoprecipitated proteins were separated in parallel in SDS-PAGE gels and transferred to polyvinylidene difluoride (PVDF) membranes. Total cellular expression of recombinant H proteins was detected using the respective Hcyt antiserum in combination with a horseradish peroxidase (HRP)-labeled secondary antiserum, while biotinylated proteins were detected using a streptavidin-HRP conjugate (Pierce) and visualized using an ECL$^+$ chemiluminescence kit (GE Healthcare). Bands were quantified using Molecular Imaging software (Kodak).

***In vivo* characterization of recombinant viruses.** Ferrets (*Mustela putoris furo*) aged 16 weeks and older (Marshall Farms) and lacking antibodies against CDV were used for all studies. All animal experiments were approved by the Animal Care and Use Committee of the INRS-Institut Armand-Frappier. Groups of five or eight ferrets were infected intranasally with 10^5 $TCID_{50}$ of the parental strain 5804PeH or strain 5804PeH$_{EpR\text{-}blind}$, respectively. Body temperature and clinical signs were recorded daily and scored based on a scale of 0 to 2, with 0 representing no change, 1 representing moderate disease, and 2 representing severe disease. Blood samples were collected from the jugular veins of animals under general anesthesia twice weekly for the first 2 weeks and weekly thereafter. Cell-associated viremia in peripheral blood mononuclear cells (PBMC) was quantified by a limiting dilution method (36), and the percentage of EGFP-expressing cells was determined by flow cytometry. The extent of PBMC proliferation inhibition was assessed by stimulation of Ficoll-purified PBMC with 1 μg/ml phytohemagglutinin (PHA) and subsequent detection of bromodeoxyuridine (BrdU) incorporation into proliferating cells by use of a cell proliferation BrdU enzyme-linked immunosorbent assay (ELISA) kit (Roche). Wild-type virus infection results include previously published data obtained from three animals (27). Two animals of each group were sacrificed on day 7 postinfection, and three were sacrificed on day 12 postinfection, to assess dissemination and to harvest tissues for histological analysis. On day 12, throat swabs were collected in 0.5 ml Opti-MEM (Invitrogen) with double-concentrated penicillin and streptomycin (Invitrogen), and urine was collected aseptically from the bladder with a needle and syringe. Virus titers were quantified by a limiting dilution method and expressed as $TCID_{50}$/ml.

Immunohistochemistry of ferret tissues. For immunohistochemistry staining, paraffin sections were deparaffinized and rehydrated following standard immunohistochemistry protocols. Endogenous peroxidase was quenched with 0.3% H_2O_2 in PBS for 12 min. After blocking with a 1:50 dilution of goat serum in PBS, the primary anti-CDV N monoclonal antibody (CDV-NP; VMRD) was added for 1 h at room temperature, followed successively by a biotinylated goat anti-mouse secondary antibody and a peroxidase-labeled streptavidin conjugate (Vector Laboratories) for 45 min each at room temperature. Infected cells were visualized using 3,3′-diaminobenzidine (DAB) substrate (Sigma), and slides were counterstained with hematoxylin.

For the detection of different cell types, cryosections of paraformaldehyde-fixed OCT-embedded tissues were thawed, permeabilized with 0.1% Triton X-100 in PBS for 10 min, and blocked with 1:50-diluted goat serum in PBS for 30 min. The slides were then incubated with either a CD3 (sc-20047; Santa Cruz) or pan-cytokeratin (C2562; Sigma) antibody for 1 h, followed by a goat anti-mouse Alexa Fluor 568-labeled secondary antiserum (Invitrogen). The slides were counterstained with 4′,6-diamidino-2-phenylindole (DAPI; Invitrogen) and mounted in Vectamount (Vector Laboratories).

RESULTS

The CDV H P493S/Y539A double mutant is EpR blind while retaining wild-type SLAM-mediated fusion efficacy. To generate an EpR-blind CDV, the MeV IC323 and CDV 5804P H proteins were aligned, and the V478S, P493S, and Y539A mutations, which correspond to the L482S, P497S, and Y543A mutations that confer the nectin-4-blind phenotype in MeV H (13), were introduced into a CDV H expression plasmid (Fig. 1A). Two of these positions, V478 and Y539, were recently identified independently as relevant to EpR in a CDV H protein alanine scanning mutagenesis study (10), thereby validating our approach. Alteration of position 493 resulted in a 70% reduction of surface expression (Fig. 1B) as detected by cell surface biotinylation. A similar reduction in

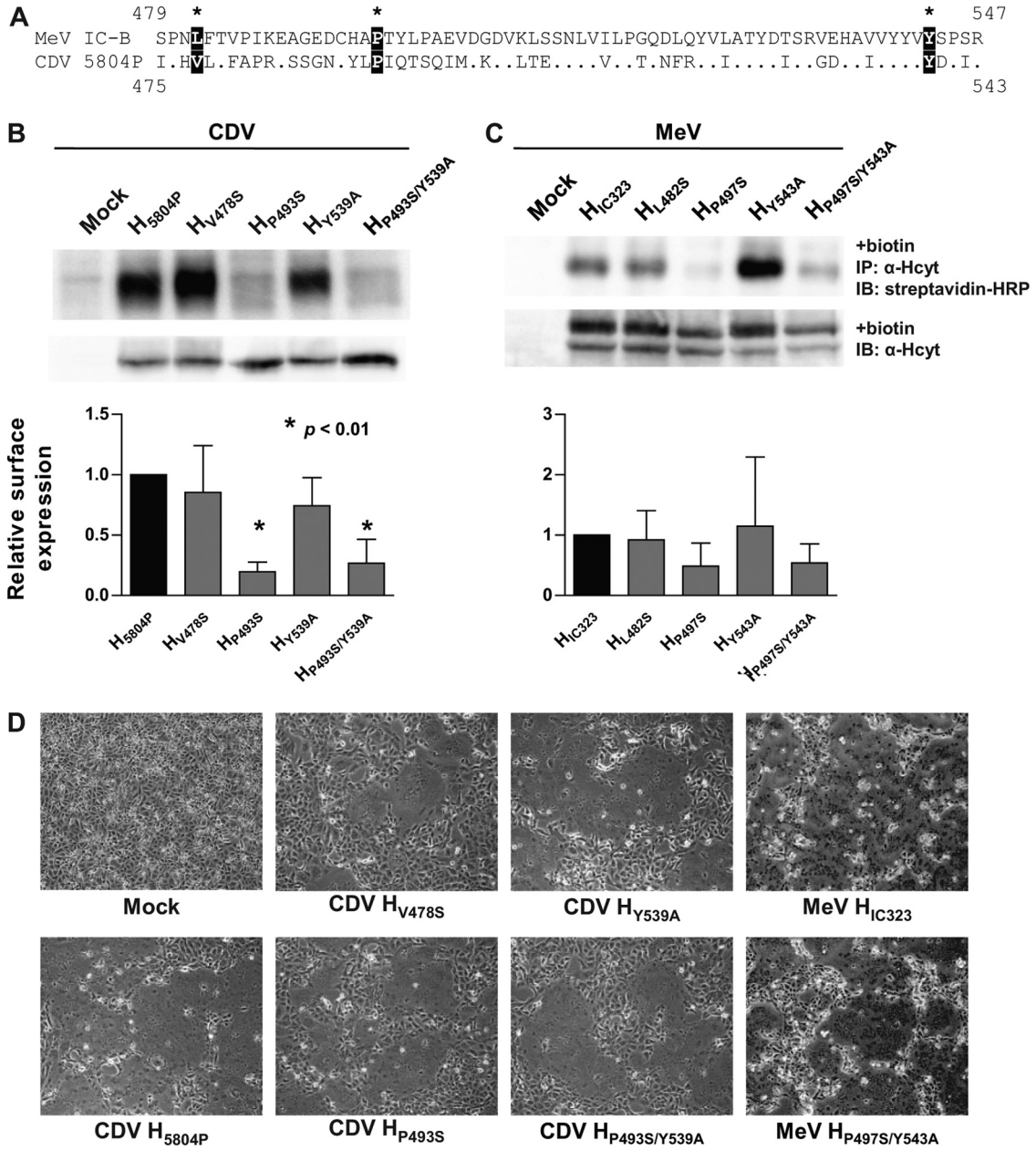

FIG 1 Transport and function of mutant H proteins. (A) Amino acid alignment of the MeV IC-B H protein and the corresponding region of the CDV 5804P H protein. Residues identified by Leonard et al. (13) (L482, P497, and Y543) as important for interaction of MeV H with nectin-4 are highlighted with asterisks above the residues. The corresponding residues (V478, P493, and Y539) were mutated in 5804P H. (B and C) Cell surface biotinylation of CDV and MeV H proteins. Cells transfected with expression plasmids for CDV (B) or MeV (C) parental and mutant H proteins were labeled with NHS-LC-LC-biotin, immunoprecipitated with an antiserum recognizing either the MeV H or CDV H protein cytoplasmic tail, and detected with a streptavidin-HRP conjugate. Western blots of cell lysates from the same experiment were analyzed for total H protein expression. The relative surface expression of each protein was calculated by normalizing the biotinylation or Western blot signal to the signal obtained for the respective parental H protein. The relative surface expression represents the ratio between the normalized biotinylation signal and the normalized Western blot signal for each replicate. Average relative surface expression levels were calculated from four independent experiments and are shown in bar graphs below the blots. (D) Cell-cell fusion observed for wild-type and mutant CDV or MeV H proteins. Confluent monolayers of VerodogSLAMtag cells were transfected with the respective H protein plasmid and the corresponding CDV or MeV F protein expression plasmid. Pictures were taken at 24 h posttransfection. Magnification, ×100.

surface expression was observed for the corresponding MeV P497S mutant (Fig. 1C), as well as the CDV and MeV H proteins carrying double mutations (P493S/Y539A for CDV H and P497S/Y543A for MeV H) (Fig. 1B and C), indicating that the proline residue at position 493/497 is important for H protein transport. However, none of the mutations significantly affected the level of cell-to-cell fusion in VerodogSLAMtag cells when the respective H proteins were coexpressed with either the MeV Edmonston (3) or CDV 5804P fusion (F) protein (Fig. 1D).

Since none of the carnivore epithelial cell lines used for the

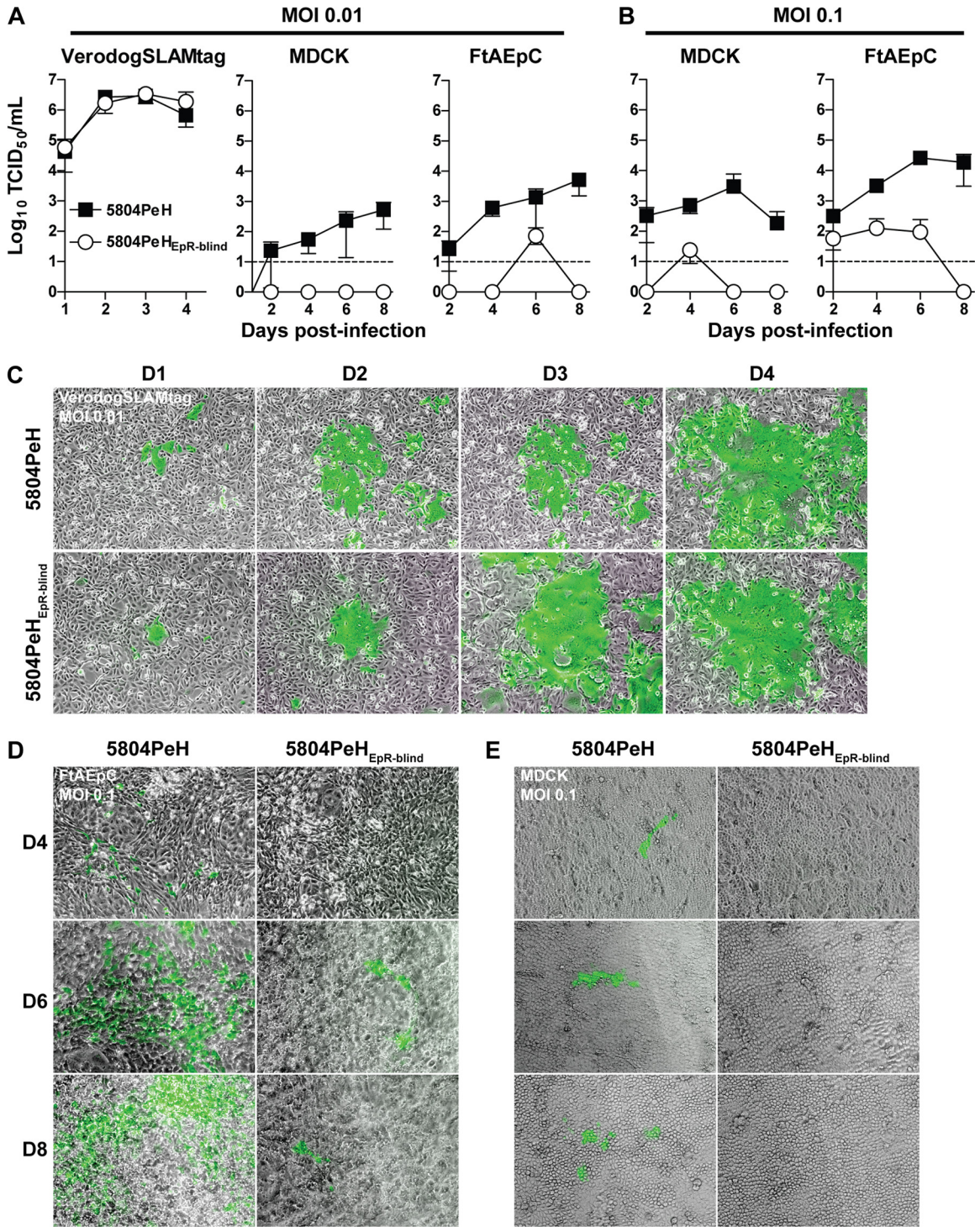

FIG 2 Characterization of recombinant viruses. (A and B) Growth kinetics in VerodogSLAMtag and MDCK cells and FtAEpCs. Cells were infected at an MOI of 0.01 (A) or 0.1 (B), and samples were collected daily for 4 days for VerodogSLAMtag cells or every second day for 8 days for epithelial cell lines. The cell-associated virus titer was determined by a limiting dilution method and expressed as the $TCID_{50}$. The average values for 4 experiments are shown, and error bars indicate standard deviations. Each dotted line represents the detection limit of the assay. (C to E) Syncytium formation in VerodogSLAMtag cells infected at an MOI of 0.01 (C) and in FtAEpCs (D) and MDCK cells (E) infected at an MOI of 0.1. Photographs were taken at the indicated time points, using fluorescence excitation and phase-contrast. Magnification, ×100. Overlays of both types of photograph are shown.

fusion assay revealed syncytium formation when wild-type or mutant CDV H proteins were coexpressed with the F protein, it was not possible to assess the extent of fusion support of the recombinant H proteins outside the viral context. We thus introduced the individual point mutations as well as the P493S/Y543A double mutation into the CDV wild-type strain 5804PeH. This virus expresses the EGFP gene from an additional open reading frame located between the H and polymerase genes (33), allowing direct

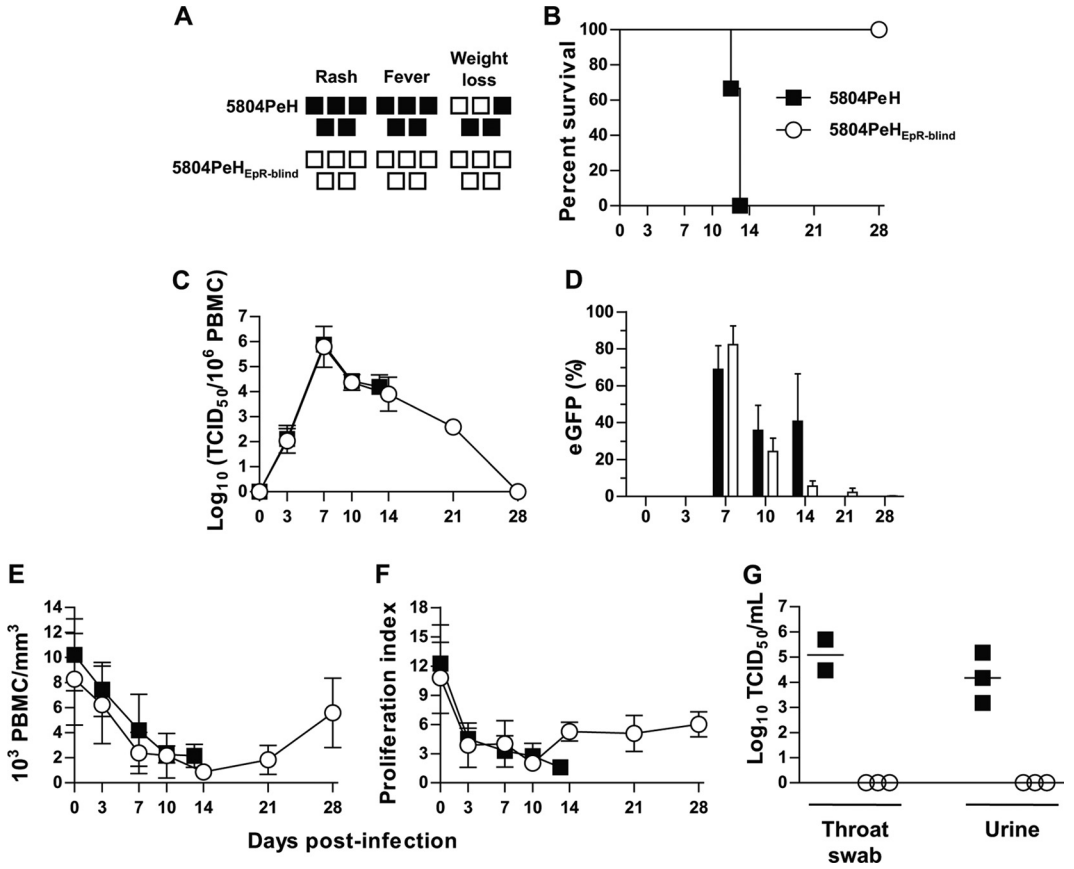

FIG 3 Pathogenesis of recombinant CDVs in ferrets. Groups of five and eight animals were infected intranasally with 10^5 $TCID_{50}$ of the parental strain 5804PeH and the recombinant virus 5804PeH$_{EpR-blind}$, respectively. Previously published data for three 5804PeH-infected animals (16) were also included, resulting in a group of eight animals for each virus. Only data for the five animals followed until day 12 after infection and until death are shown in panels A and B, respectively. (A) Clinical scores observed for wild-type virus- and 5804PeH$_{EpR-blind}$-infected animals. Scores are shown for the five animals followed until day 12 after infection or until death. Each square represents one animal. White squares indicate no changes, and black squares indicate severe rash, fever above 40°C, and weight loss above 10%. (B) Survival of animals infected with the different viruses. The death of an animal is indicated by a step down on the curve. (C) The course of cell-associated viremia is shown as the $\log_{10}$ of the virus titer per 10^6 PBMC. (D) The percentage of infected PBMC was quantified by flow cytometry. (E) Total leukocyte counts from infected animals, shown as 10^3 leukocytes per mm^3. (F) *In vitro* proliferation activity of lymphocytes from infected animals. Days postinfection are indicated on the *x* axes of the graphs, and error bars represent standard deviations. (G) Quantification of virus shedding in epithelial tissues on day 12 after infection. Titers are expressed as $TCID_{50}$/ml. Each symbol represents one animal, and geometric means are indicated by horizontal black lines.

visualization of infected cells. While each of the individual mutations resulted in a reduction of epithelial cell infection efficiency (data not shown), only the double mutant previously identified in the MeV system was unable to infect epithelial cells and was thus chosen for further characterization.

The wild-type and 5804PeH$_{EpR-blind}$ viruses replicated to similar maximum titers in VerodogSLAMtag cells (Fig. 2A, left panel). Both viruses induced the formation of syncytia of comparable sizes (Fig. 2C), illustrating that the reduced cell surface expression associated with the P497S mutation did not affect fusion efficiency or overall viability in the context of SLAM-mediated infection. In contrast, only the wild-type virus replicated efficiently in MDCK cells and FtAEpCs (Fig. 2A and B). Even at a 10-fold-higher MOI, 5804PeH$_{EpR-blind}$ resulted in only a few infected foci and in titers slightly above the detection level at some of the time points (Fig. 2B, D, and E). Thus, the transfer of the mutations involved in MeV interaction with nectin-4 to CDV resulted in the expected EpR-blind phenotype.

5804PeH$_{EpR-blind}$ causes severe immunosuppression but no clinical disease. To assess the importance of spread to epithelial tissues for morbillivirus pathogenesis, ferrets were infected intranasally with 10^5 $TCID_{50}$ of the parental strain 5084PeH or strain 5804PeH$_{EpR-blind}$. In contrast to the case with 5804PeH-infected animals, which developed severe rash and fever and died within 12 days after infection, the EpR-blind virus did not elicit fever and caused no clinical signs of disease (Fig. 3A and B). Fluorescence imaging revealed a few weakly GFP-expressing spots around the mouths and eyes as the only indication of 5804PeH$_{EpR-blind}$ infection, while the wild-type virus resulted in extensive fluorescence of all mucosal surfaces and caused the typical skin rash (33; data not shown). Despite these differences in pathogenesis, both viruses resulted in similar kinetics of cell-associated viremia (Fig. 3C), with 70 to 90% of PBMC infected 7 days after inoculation (Fig. 3D), indicating that the epithelial cell receptor-blind virus was not affected in the ability to infect immune cells and spread throughout the lymphatic system. All animals also developed strong leukopenia, resulting in an 80% reduction in leukocytes at day 10 after infection (Fig. 3E). Finally, infection with both viruses resulted in a 75% inhibition of lymphocyte proliferation activity (Fig. 3F). Thus, the values of these two indicators of morbillivirus

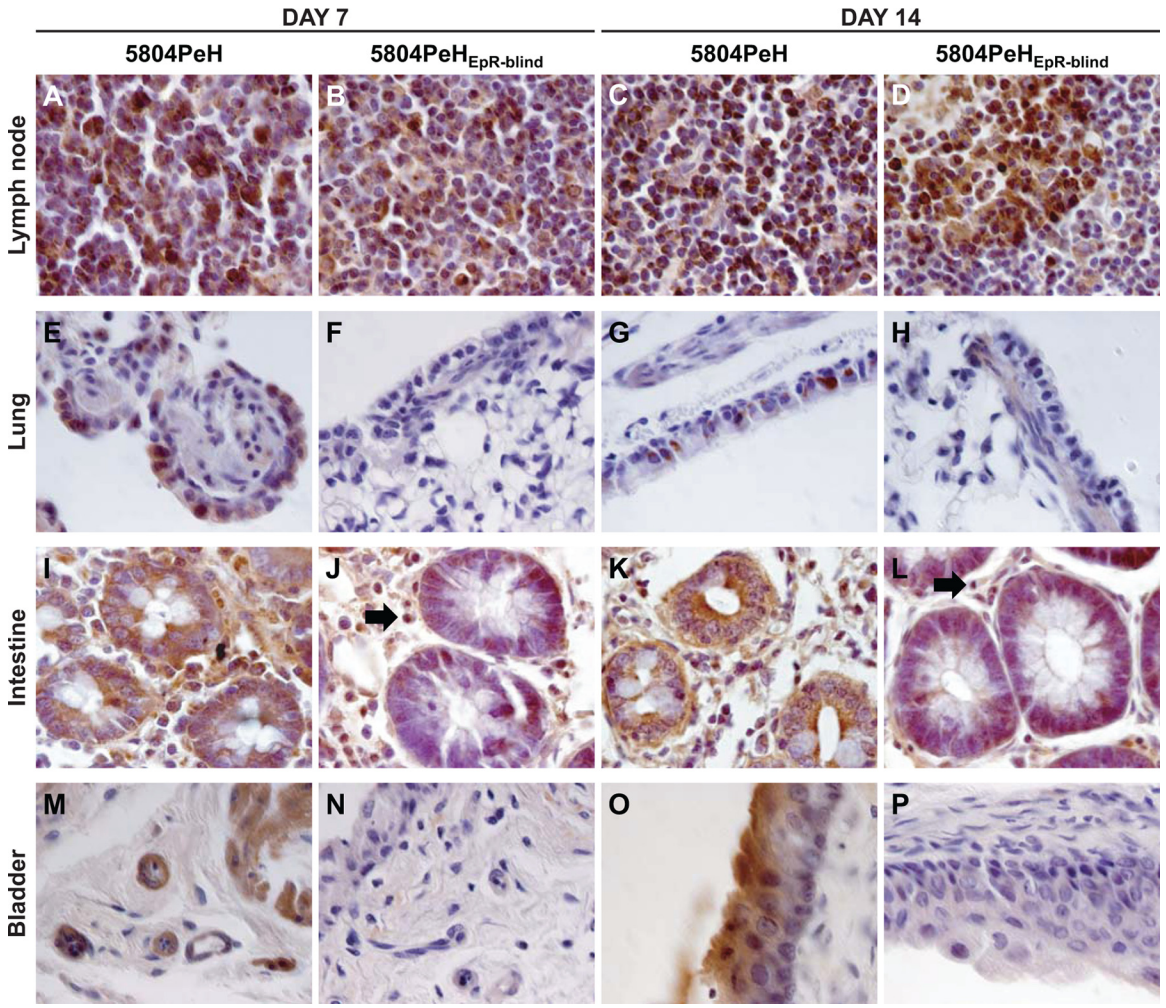

FIG 4 Immunohistochemical detection of CDV in ferret lymphatic and epithelial tissues. (A to D) Lymph node sections from animals infected with either 5804PeH (A and C) or 5804PeH$_{EpR-Blind}$ (B and D) and sacrificed at either day 7 (A and B) or day 12 (C and D) postinoculation. (E to H) Lung sections from animals infected with either 5804PeH (E and G) or 5804PeH$_{EpR-blind}$ (F and H) and sacrificed at either day 7 (E and F) or day 14 (G and H) postinfection. (I to L) Intestinal sections from animals infected with either 5804PeH (I and K) or 5804PeH$_{EpR-blind}$ (J and L) and sacrificed at either day 7 (I and J) or day 14 (K and L) postinfection. Black arrows in panels J and L indicate infected cells that are of lymphoid morphology. (M to P) Bladder sections from animals infected with either 5804PeH (M and O) or 5804PeH$_{EpR-blind}$ (N and P) and sacrificed at either day 7 (M and N) or day 14 (O and P) postinfection. All pictures were taken at a magnification of ×1,000, under oil immersion.

immunosuppression (7, 24) were equivalent for the first 10 days of infection. Even though recovery of the white blood cell count and lymphocyte proliferation activity in 5804PeH$_{EpR-blind}$-infected animals correlated to a certain extent with virus clearance, preinfection levels were not reached during the duration of the experiment.

To investigate the importance of epithelial cell infection for shedding, three additional animals were infected with each virus, and throat swabs and urines were collected on day 12 after infection. While high titers were detected in samples from wild-type virus-infected animals, no virus was found in samples from the EpR-blind virus group (Fig. 3G). Thus, the EpR-blind CDV remained immunosuppressive but did not cause disease and was not shed.

5804PeH$_{EpR-blind}$ is not detected in epithelial tissues. Immunohistochemical staining of paraformaldehyde-fixed paraffin-embedded tissue sections from animals sacrificed on day 7 or 12 after infection, using a CDV nucleoprotein-specific monoclonal antibody, revealed similar infection levels in the intestinal lymph nodes (Fig. 4A to D) and other immune tissues (data not shown). In contrast, CDV-positive epithelial cells were found only in tissues from animals infected with wild-type virus (Fig. 4E to P), with infection levels increasing over time. Occasional infected cells detected in epithelial tissues of EpR-blind virus-infected animals were all of lymphoid morphology (Fig. 4J and L, arrows), and staining of paraformaldehyde-fixed cryosections (which maintained EGFP expression in infected cells) with antibodies for T cells or epithelial cells confirmed that most infected cells were indeed immune cells (Fig. 5). Taken together, these results suggest that infection of epithelial tissues is essential for clinical disease and shedding but has minimal, if any, influence on immunosuppression.

DISCUSSION

After transmission by aerosol, morbilliviruses cross the respiratory epithelium to reach immune tissues via infected immune cells, most likely macrophages or dendritic cells (6, 11, 13, 33).

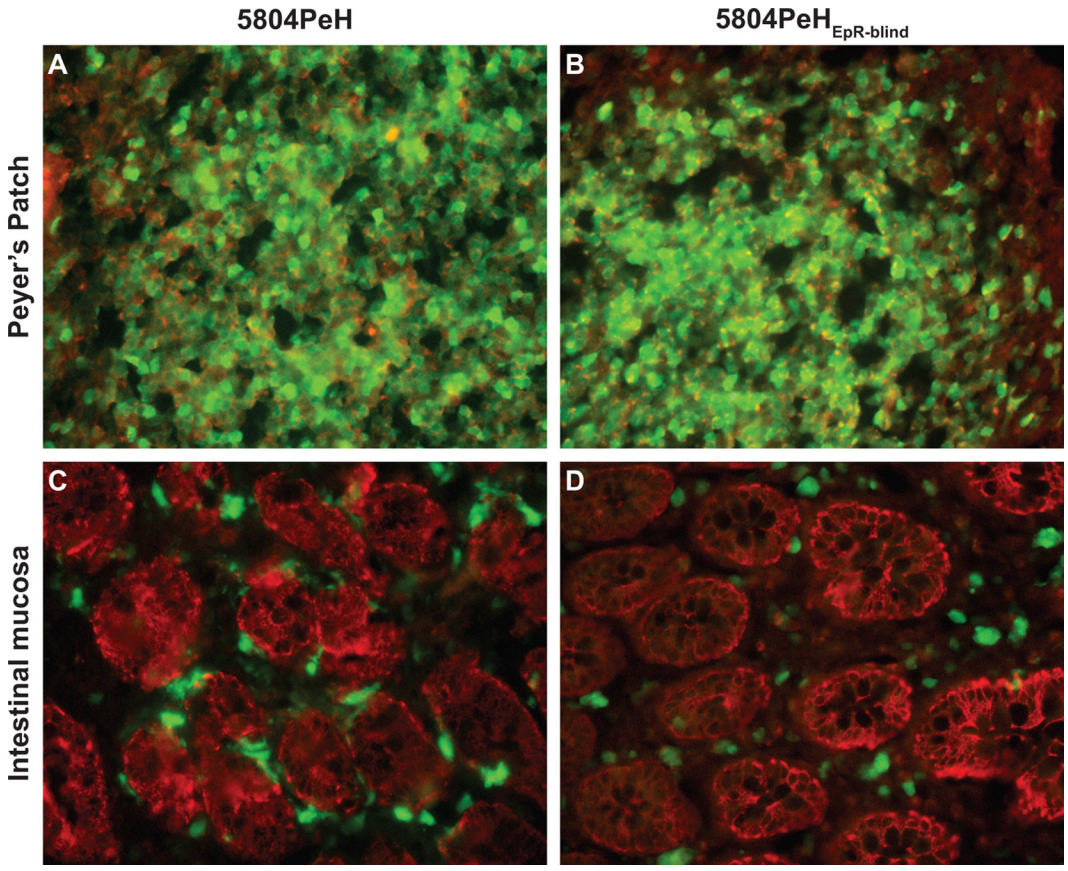

FIG 5 Immunohistochemical staining of infected immune and epithelial cells. Paraformaldehyde-fixed cryosections of Peyer's patches and small intestine harvested on day 7 after infection with 5804PeH (A and C) or 5804PeH$_{\text{EpR-blind}}$ (B and D) were stained with markers for T cells (CD3; Santa Cruz) (A and B) or cytokeratin (C2562; Sigma) (C and D), followed by an Alexa Fluor 568-labeled secondary antiserum. Nuclei were counterstained with DAPI.

Nevertheless, since it is conceivable that epithelial cell infection sustains virulence in late infection stages, we sought to confer an EpR-blind phenotype to an extremely virulent CDV strain that is lethal for ferrets. To this end, we transferred the MeV H P497S/Y543A double mutation, which results in a nectin-4-blind MeV (13, 17), into the CDV 5804PeH H protein. The resulting recombinant virus efficiently infected and replicated in SLAM-expressing Vero cells but was severely impaired in the ability to infect canine or ferret epithelial cell lines. In ferrets, the EpR-blind CDV was initially indistinguishable from the wild-type virus, reaching similar infection levels and causing severe leukopenia and inhibition of lymphocyte proliferation. However, the virus was completely attenuated, and there was no shedding. Immunohistochemistry staining confirmed the EpR-blind phenotype *in vivo*, indicating that epithelial cell infection is critical for clinical morbillivirus disease.

Immune cell infection alone is sufficient to induce prolonged immunosuppression. Severe acute and, in many cases, long-lasting immunosuppression is a hallmark of morbillivirus infections (7). During the acute phase, morbillivirus immunosuppression is characterized by an often dramatic leukopenia and an inability of PBMC to proliferate upon stimulation (18, 25, 28), and the extent of both parameters correlates with disease severity (21, 28, 38). However, while leukocyte counts recover rapidly after virus clearance (16, 22), the inhibition of lymphocyte proliferation frequently persists beyond clinical recovery (8, 38). The wild-type levels of leukopenia and inhibition of lymphocyte proliferation we saw in animals infected with the EpR-blind virus now demonstrate that acute immunosuppression is primarily a consequence of immune cell infection and can occur independently from clinical disease. Our findings are supported by the leukopenia and inhibition of lymphocyte proliferation observed in knock-in mice expressing murine SLAM with a human V domain (20), which carries the MeV H-interacting residues (23), since MeV is *de facto* EpR blind in these animals due to the lack of appropriate receptors in cells other than the SLAM-expressing immune cells. The prolonged inhibition of lymphocyte proliferation activity in the absence of clinical disease in ferrets infected with the EpR-blind CDV further suggests that this virus provides a unique opportunity to investigate mechanisms underlying prolonged morbillivirus immunosuppression and its impact on susceptibility to secondary infections.

Epithelial cell infection is not required for initial infection and dissemination but is essential for clinical disease and shedding. Consistent with a previous report of a nectin-4-blind MeV reaching wild-type titers in PBMC from infected rhesus monkeys (13), the EpR-blind CDV replicated with wild-type kinetics in ferret PBMC and attained similar infection levels. Taken together with the lack of viremia and disease progression associated with SLAM-blind viruses (12, 36), these results further illustrate that

epithelial cell infection plays little to no role in the initial stages of morbillivirus pathogenesis.

In wild-type and nectin-4-blind MeV-infected rhesus macaques, similar rash frequencies and severities, but no other clinical signs, were reported (13). In contrast, we observed only a few EGFP-expressing spots at the lips and eyes of ferrets infected with the EpR-blind virus, while the wild-type virus was associated with severe rash. Since studies with EGFP-expressing MeV in cynomolgus macaques demonstrated that the rash represents infected immune cells in the skin rather than infected skin cells (4), the occasionally observed EGFP-positive foci in EpR-blind virus-infected ferrets may thus likely be attributed to immune cell infection, while the more severe manifestation seen in wild-type virus-infected animals reflects spread to epithelial skin cells. We previously reported a correlation between the onset of rash and clinical signs and the spread to epithelial tissues (33), and septicemia due to disruption of epithelial barriers in the intestine has long been considered the most likely immediate cause of death for CDV-infected ferrets. The results presented here clearly establish epithelial cell infection as the cause of clinical disease by CDV and, likely, by morbilliviruses in general. Furthermore, the absence of virus in tracheal aspirates of monkeys (13) and throat swabs and urines of ferrets infected with EpR-blind viruses suggests that epithelial cell infection is necessary for shedding and ultimate spread to new hosts. Therapeutic interventions that aim to interrupt the dissemination to epithelial tissues may thus not only protect from clinical disease but also prevent transmission.

Morbillivirus H protein residues important for epithelial cell infection are conserved. Epithelial cell infection is an integral part, to various extents, of morbillivirus pathogenesis (7). Several of the MeV H protein amino acids involved in binding to the recently discovered epithelial cell receptor nectin-4 (13, 17, 19, 29) were found to also be essential for CDV epithelial cell infection in an independent alanine scanning mutagenesis study of the corresponding CDV H protein region (10). Here we show that introduction of the two key mutations into the H protein of a wild-type CDV strain resulted in an EpR-blind phenotype *in vitro* and *in vivo*. While the role of nectin-4 as a receptor for CDV remains to be demonstrated, the involvement of the same H protein residues in MeV and CDV epithelial cell infections strongly suggests that the epithelial cell receptor, similar to the immune cell receptor SLAM (31), is conserved among morbilliviruses.

ACKNOWLEDGMENTS

We thank Michael Mühlebach and all laboratory members for helpful discussions.

This work was supported by grants from the CIHR (MOP-66989), NSERC (299385-04), and CFI (9488) to V.V.M. and by NIH grant R01 AI63476 to R.C. X.-X.W. was supported by scholarships from the Armand-Frappier Foundation and the CIHR.

REFERENCES

1. **Anderson DE, von Messling V.** 2008. The region between the canine distemper virus M and F genes modulates virulence by controlling fusion protein expression. J. Virol. **82**:10510–10518.
2. **Barrett T.** 1999. Morbillivirus infections, with special emphasis on morbilliviruses of carnivores. Vet. Microbiol. **69**:3–13.
3. **Cathomen T, Buchholz CJ, Spielhofer P, Cattaneo R.** 1995. Preferential initiation at the second AUG of the measles virus F mRNA: a role for the long untranslated region. Virology **214**:628–632.
4. **De Swart RL, et al.** 2007. Predominant infection of $CD150^+$ lymphocytes and dendritic cells during measles virus infection of macaques. PLoS Pathog. **3**:e178.
5. **de Vries RD, et al.** 2010. *In vivo* tropism of attenuated and pathogenic measles virus expressing green fluorescent protein in macaques. J. Virol. **84**:4714–4724.
6. **Ferreira CSA, et al.** 2010. Measles virus infection of alveolar macrophages and dendritic cells precedes spread to lymphatic organs in transgenic mice expressing human signaling lymphocytic activation molecule (SLAM, CD150). J. Virol. **84**:3033–3042.
7. **Griffin DE.** 2007. Measles virus, p 1551–1586. *In* Knipe DM, et al (ed), Fields virology, 5th ed. Lippincott Williams & Wilkins, Philadelphia, PA.
8. **Krakowka S, Cockerell G, Koestner A.** 1975. Effects of canine distemper virus infection on lymphoid function in vitro and in vivo. Infect. Immun. **11**:1069–1078.
9. **Kugel D, et al.** 2009. Intranasal administration of alpha interferon reduces seasonal influenza A virus morbidity in ferrets. J. Virol. **83**:3843–3851.
10. **Langedijk JPM, et al.** 2011. Canine distemper virus infects canine keratinocytes and immune cells by using overlapping and distinct regions located on one side of the attachment protein. J. Virol. **85**:11242–11254.
11. **Lemon K, et al.** 2011. Early target cells of measles virus after aerosol infection of non-human primates. PLoS Pathog. **7**:e1001263.
12. **Leonard VHJ, Hodge G, Reyes-del Valle J, McChesney MB, Cattaneo R.** 2010. Measles virus selectively blind to signaling lymphocytic activation molecule (SLAM; CD150) is attenuated and induces strong adaptive immune responses in rhesus monkeys. J. Virol. **84**:3413–3420.
13. **Leonard VHJ, et al.** 2008. Measles virus blind to its epithelial cell receptor remains virulent in rhesus monkeys but cannot cross the airway epithelium and is not shed. J. Clin. Invest. **118**:2448–2458.
14. **Martin A, Staeheli P, Schneider U.** 2006. RNA polymerase II-controlled expression of antigenomic RNA enhances the rescue efficacies of two different members of the *Mononegavirales* independently of the site of viral genome replication. J. Virol. **80**:5708–5715.
15. **McChesney MB, et al.** 1997. Experimental measles. I. Pathogenesis in the normal and the immunized host. Virology **233**:74–84.
16. **McCullough B, Krakowka S, Koestner A.** 1974. Experimental canine distemper virus-induced lymphoid depletion. Am. J. Pathol. **74**:155–170.
17. **Mühlebach MD, et al.** 2011. Adherens junction protein nectin-4 is the epithelial receptor for measles virus. Nature **480**:530–533.
18. **Nielsen L, et al.** 2009. Lymphotropism and host responses during acute wild-type canine distemper virus infections in a highly susceptible natural host. J. Gen. Virol. **90**:2157–2165.
19. **Noyce RS, et al.** 2011. Tumor cell marker PVRL4 (nectin 4) is an epithelial cell receptor for measles virus. PLoS Pathog. **7**:e1002240.
20. **Ohno S, et al.** 2007. Measles virus infection of SLAM (CD150) knockin mice reproduces tropism and immunosuppression in human infection. J. Virol. **81**:1650–1659.
21. **Okada H, et al.** 2000. Extensive lymphopenia due to apoptosis of uninfected lymphocytes in acute measles patients. Arch. Virol. **145**:905–920.
22. **Okada H, et al.** 2001. Comparative analysis of host responses related to immunosuppression between measles patients and vaccine recipients with live attenuated measles vaccines. Arch. Virol. **146**:859–874.
23. **Ono N, Tatsuo H, Tanaka K, Minagawa H, Yanagi Y.** 2001. V domain of human SLAM (CDw150) is essential for its function as a measles virus receptor. J. Virol. **75**:1594–1600.
24. **Pillet S, Svitek N, von Messling V.** 2009. Ferrets as a model for morbillivirus pathogenesis, complications, and vaccines. Curr. Top. Microbiol. Immunol. **330**:73–87.
25. **Ryon JJ, Moss WJ, Monze M, Griffin DE.** 2002. Functional and phenotypic changes in circulating lymphocytes from hospitalized Zambian children with measles. Clin. Diagn. Lab. Immunol. **9**:994–1003.
26. **Sawatsky B, Grolla A, Kuzenko N, Weingartl H, Czub M.** 2007. Inhibition of henipavirus infection by Nipah virus attachment glycoprotein occurs without cell surface down-regulation of ephrin-B2 or ephrin-B3. J. Gen. Virol. **88**:582–591.
27. **Sawatsky B, von Messling V.** 2010. Canine distemper viruses expressing a hemagglutinin without N-glycans lose virulence but retain immunosuppression. J. Virol. **84**:2753–2761.
28. **Svitek N, von Messling V.** 2007. Early cytokine mRNA expression profiles predict morbillivirus disease outcome in ferrets. Virology **362**:404–410.
29. **Tahara M, et al.** 2008. Measles virus infects both polarized epithelial and immune cells by using distinctive receptor-binding sites on its hemagglutinin. J. Virol. **82**:4630–4637.
30. **Takeda M, et al.** 2000. Recovery of pathogenic measles virus from cloned cDNA. J. Virol. **74**:6643–6647.

31. **Tatsuo H, Ono N, Yanagi Y.** 2001. Morbilliviruses use signaling lymphocyte activation molecules (CD150) as cellular receptors. J. Virol. **75**:5842–5850.
32. **Vongpunsawad S, Oezgun N, Braun W, Cattaneo R.** 2004. Selectively receptor-blind measles viruses: identification of residues necessary for SLAM- or CD46-induced fusion and their localization on a new hemagglutinin structural model. J. Virol. **78**:302–313.
33. **von Messling V, Milosevic D, Cattaneo R.** 2004. Tropism illuminated: lymphocyte-based pathways blazed by lethal morbillivirus through the host immune system. Proc. Natl. Acad. Sci. U. S. A. **101**:14216–14221.
34. **von Messling V, et al.** 2005. Nearby clusters of hemagglutinin residues sustain SLAM-dependent canine distemper virus entry in peripheral blood mononuclear cells. J. Virol. **79**:5857–5862.
35. **von Messling V, Springfeld C, Devaux P, Cattaneo R.** 2003. A ferret model of canine distemper virus virulence and immunosuppression. J. Virol. **77**:12579–12591.
36. **von Messling V, Svitek N, Cattaneo R.** 2006. Receptor (SLAM [CD150]) recognition and the V protein sustain swift lymphocyte-based invasion of mucosal tissue and lymphatic organs by a morbillivirus. J. Virol. **80**:6084–6092.
37. **von Messling V, Zimmer G, Herrler G, Haas L, Cattaneo R.** 2001. The hemagglutinin of canine distemper virus determines tropism and cytopathogenicity. J. Virol. **75**:6418–6427.
38. **Ward BJ, Johnson RT, Vaisberg A, Jauregui E, Griffin DE.** 1991. Cytokine production *in vitro* and the lymphoproliferative defect of natural measles virus infection. Clin. Immunol. Immunopathol. **61**:236–248.